

REVIEWS OF MODERN PHYSICS

VOLUME 45, NUMBER 3

JULY 1973

Photoabsorption and Charge Oscillation of the Thomas-Fermi Atom*†

J. A. Ball[‡], J. A. Wheeler, and E. L. Fireman[§]

Joseph Henry Laboratories, Princeton University, Princeton, New Jersey 08540

The complications of calculating the photoabsorption cross section of atoms for frequencies in the far ultraviolet and soft x-ray regions motivate an analysis of this problem on the basis of the Bloch semiclassical model of hydrodynamic charge oscillation in the neutral Thomas-Fermi atom. The hydrodynamic modes of oscillation of the neutral Thomas-Fermi atom have a continuous frequency spectrum. The resulting photoabsorption cross section is a continuous function of frequency which scales with atomic number Z and in this sense is a universal cross section, approximately applicable to all heavy atoms. Numerical solutions of the normal mode functions of dipole charge oscillation are used to calculate the photoabsorption cross section in a range of photon energies $0.816 Z \text{ eV} < \hbar\omega < 272 Z \text{ eV}$, the range where the model is expected to be most realistic. In this range the semiclassical hydrodynamic cross section agrees with experimental data for the noble gases as well as could be expected for a cross section applicable to all atoms. The model cross section, extended to zero and infinite frequencies by analytical calculation, checks the sum rule to within 2%; but gives a value $I = 4.95 Z \text{ eV}$ for the logarithmic mean excitation energy of stopping power formulas. The unrealistically low value of I/Z results because the Thomas-Fermi atom exaggerates the number of electrons which absorb at low frequencies. Use of the hydrodynamic cross section in the approximate range of validity of this model $\hbar\omega > 0.816 Z \text{ eV}$ gives $I = 12.4e^\beta Z \text{ eV}$, where β depends upon the oscillator strength below $\hbar\omega = 0.816 Z \text{ eV}$ which cannot be satisfactorily determined from the Bloch model. Used within its limitations the Bloch model of hydrodynamic oscillation in the statistical atom provides a useful method of estimating photoabsorption cross sections and could possibly be applied to other atomic processes.

CONTENTS

1. Introduction.....	333
2. Hydrodynamic Oscillations of the Thomas-Fermi Atom..	335
2.1. Normal Mode of Oscillation.....	336
2.2. Oscillation Energy and the Photoabsorption Cross Section.....	338
3. Numerical Calculations and Results of the Hydrodynamic Model.....	339
3.1. Comparison with Experiment.....	341
3.2. Oscillator Strength and Sum Rule.....	341
3.3. Limits of Cross Section at Extremes of Frequency.....	341
3.4. Check of Sum Rule.....	342
3.5. The Logarithmic Mean Excitation Energy.....	342
4. Conclusion.....	343
Appendix A: Numerical Solution of the Coupled Hydrodynamic Equations.....	343
Appendix B: Evaluation of the Dipole Integral.....	350

1. INTRODUCTION

Of all the features of atomic physics none does more than the photoabsorption cross section as a function of frequency, $\sigma(\omega)$, to reveal in compact compass the principal feature of the electronic binding; and of all domains of the frequency ω in none is the mechanism of absorption more clearly a many-electron process

than in the range between the bindings of the outermost electrons and the bindings of the innermost electrons,

$$me^4/\hbar^3 \ll \omega \ll Z^2 me^4/\hbar^3.$$

At high frequencies ($\hbar\omega \approx Z^2$ times 13.6 eV) the characteristic K and L absorption edges take their origin in only a small number of electrons and are susceptible to simple theoretical analysis. At low frequencies ($\hbar\omega$ of the order of and less than 13.6 eV) in the optical part of the spectrum, the photoabsorption is again due to only a few of the many atomic electrons. The binding of these electrons varies from element to element, reflecting the filling of different electron shells and subshells. It is impossible to describe the absorption in the optical region, even approximately, by a simple formula valid for all atoms. At both high and low frequencies there are evidently windows in the absorption spectrum—regions of reduced or zero cross section. The contrary is true of the region of intermediate frequencies (of the general order of Z times the Rydberg).

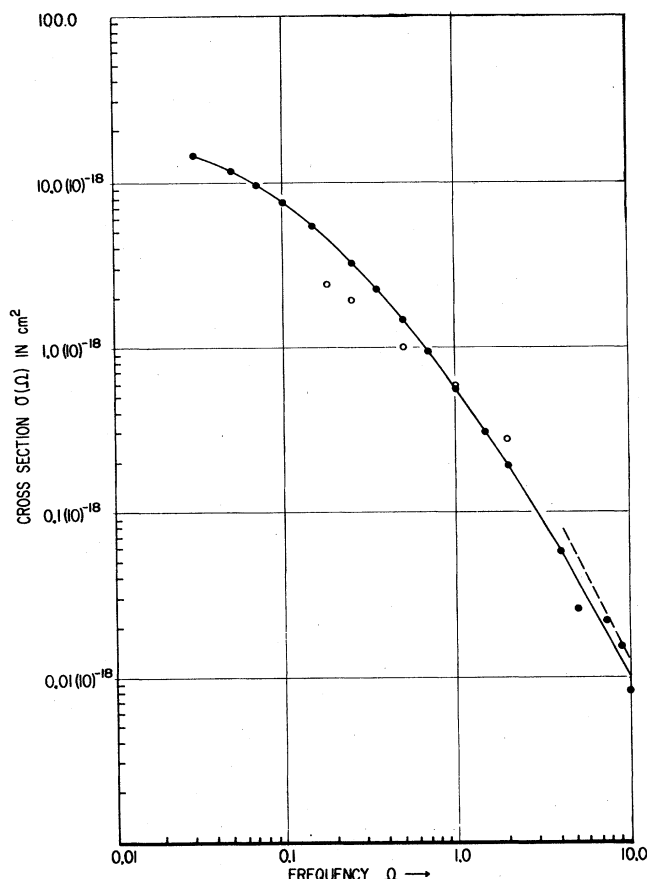


FIG. 1. The universal atomic photoabsorption cross section calculated from the Bloch hydrodynamic model of the Thomas-Fermi atom. The abscissa is the photon frequency plotted in dimensionless units $\Omega = (\text{Photon energy in eV}) / (27.2Z \text{ eV})$, where Z is the atomic number of the absorbing atom. The solid dots are the numerical values computed in this paper. The open circles are preliminary results calculated by two of the authors [Wheeler and Fireman (1957)]. The dashed line is an analytical form of the cross section which is asymptotically valid at high frequencies; cf. Appendix B.

Here the effects due to the individual electronic groups overlap and at each frequency many electrons contribute to the photoabsorption. Accurate calculations of the photoabsorption in this region require a considerable extension of the usual methods for analyzing the spectroscopic terms of a few-electron system. The complexities of calculating atomic photoabsorption at these intermediate frequencies may be appreciated by consulting the comprehensive review article of Fano and Cooper (1968). One finds it necessary to consider among other complications such effects as intrachannel interaction, core relaxation, double excitations, and gross effects of spectral repulsion.

These complications suggest that a statistical treatment of the photoabsorption in this intermediate range of frequencies would be appropriate and useful, even

though such a treatment of necessity might be only of an approximate character. Such an approach is provided by Bloch's (1933) hydrodynamic treatment of the Thomas-Fermi model of the statistical atom. Although models of photoabsorption based upon the statistical atom have been investigated before,¹ the original idea of Bloch, advanced many years ago, has never previously been worked out. In this article we solve Bloch's hydrodynamic equations for the charge oscillations of the neutral Thomas-Fermi atom and apply the solutions to the calculation of the atomic photoabsorption cross section predicted by this model.

Aside from the foregoing considerations, we took up the theory of the absorption properties of the statistical atom for another reason. Atomic physics is so completely unified by quantum mechanics that one wishes to see this unity displayed in the form of general expressions for energy release and transition probabilities for all the important processes of atomic physics. Many of these quantities when considered with all accuracy depend upon the atomic number in a complicated manner. Consequently one is ordinarily content for survey purposes to know the transition energy or cross section under consideration for the two limiting cases of hydrogen, as the simplest atom, and the Thomas-Fermi atom, as the statistical representative of all heavier atoms. Apart from atom-atom collisions which entail structural complexities of the combined system that are far from simple, this level of knowledge has been attained in the case of most elementary atomic processes. One of the most striking exceptions to date to this standard of analysis has been up to now the absence of an overall picture of the photoelectric effect for heavy atoms at intermediate frequencies.

The results of our calculation of the photoabsorption predicted by the Bloch model appear in Fig. 1 and are tabulated in Table I. It is not surprising that this analysis yields a photoabsorption cross section that is a smooth function of frequency. Such a smoothed out statistical absorption curve omits reference to all the special details of the electronic structure of any one atom. The curve can be expected to apply in about the same degree of approximation to all heavy atoms by simple change of scale. In this sense it constitutes a universal curve for the photoelectric cross section of many-electron atoms. It is important to emphasize, however, the approximate nature of this curve. Indeed today for many elements far more accurate cross sections have been determined, both experimentally and

¹ Similar considerations have motivated other authors to describe the atomic absorption in this frequency range by means of the statistical atom. See, for example, Lindhard (1954). Brandt and Lundqvist (1965, 1965a) do not solve the Bloch equations for the global response of the atom, but extend the treatment of Lindhard by treating the response in terms of the local electron density within the atom and then introduce corrections for the density gradients. Their results are qualitatively the same as ours.

theoretically. Our entire analysis of atomic hydrodynamic oscillation is based upon the neutral Thomas-Fermi atom in its original and simplest form. As discussed below in more detail many of the unrealistic features of the photoabsorption curve of Fig. 1—especially its behavior at low frequencies—can be traced to defects inherent in this simple Thomas-Fermi model. Many improvements have been added to the original (Thomas, 1926; Fermi, 1928) Thomas-Fermi atom

TABLE I. Atomic photoabsorption cross section calculated from the Bloch model of hydrodynamic oscillation of the statistical atom.

Frequency Ω^a	Dipole integral ^b $D(\Omega)$	Cross section $\sigma(\Omega)$ in 10^{-18} cm ²
0.0 ^c	$3.30\pi\Omega$	207.5
0.1 to $3(10)^{-5}$ ^d		207.5
$3(10)^{-5}$ to 0.03 ^e		$3.84/\Omega^{0.383}$
0.03	0.0831	14.78
0.05	0.1234	11.73
0.07	0.1554	9.487
0.10	0.1975	7.509
0.15	0.2503	5.360
0.25	0.3272	3.290
0.35	0.3775	2.240
0.50	0.4357	1.462
0.70	0.4851	0.9245
1.00	0.5325	0.5459
1.50	0.5908	0.2986
2.00	0.6239	0.1873
4.00	0.6884	0.05702
5.00 ^f	0.575	0.0255
7.50 ^f	0.8158	0.02278
9.00 ^f	0.788	0.01476
10.00 ^f	0.6475	0.008026
12.00 ^f	0.6623	0.005864
Very large ^g	0.805	$1.24/\Omega^2$

$$\text{Integrated value } \int_0^\infty \sigma(\Omega) d\Omega = 3.95(10)^{-18} \text{ cm}^2$$

^a Frequency parameter $\Omega = (\text{photon energy in eV}) / (27.2 Z \text{ eV})$.

^b $D(\Omega)$ is proportional to the dipole moment of the spatial distribution of charge in a normal mode. The cross section is given by

$$\sigma(\Omega) = (3\pi\alpha a_0^2 / \Omega^2) [D(\Omega)]^2,$$

where α is the fine structure constant and a_0 is the Bohr radius; cf: Appendix A.

^c Analytical result, cf. Appendix B.

^d Region of Ω so low that the bulk of absorption takes place in far out region of electron cloud, where $\varphi \approx 144/x^2$; hence same result assumed here for $\sigma(\Omega)$ as calculated at zero frequency.

^e Simplest interpolation that is at the same time qualitatively reasonable; no other justification.

^f Calculated cross sections at these frequencies may be in error by 15%.

^g Analytical result, asymptotically valid at high frequencies; cf. Appendix B.

by various authors (see, for example, March, 1951; Gombas, 1956); corrections for electron exchange and for electron correlation, corrections for large potential gradients near the nucleus, and grouping of electrons by angular momentum. A hydrodynamic analysis based upon these more realistic models of the statistical atom would perhaps yield a more accurate photoabsorption curve. However all the improved statistical models destroy the original Thomas-Fermi model's unique property of scaling with the atomic number Z in a simple way. The present analysis of the hydrodynamic oscillation of the statistical atom sacrifices some degree of detail and accuracy, but preserves this valuable scaling property.

The approximate universal cross section for photoabsorption in the far ultraviolet and soft x-ray region which we have just discussed evidently has applications in radiation physics, astrophysics, aeronomy, and plasma physics. It provides an approximate photoabsorption cross section in those cases where more accurate cross sections are lacking. In particular, a knowledge of the dependence of absorption on frequency also allows one to estimate the logarithmic mean excitation energy, I , which enters into the standard equation^{2,3} for the stopping power of matter for swift charged particles,

$$\ln I \equiv \langle \ln \hbar\omega \rangle_{av} = \int_0^\infty (\ln \hbar\omega) \sigma(\omega) d\omega / \int_0^\infty \sigma(\omega) d\omega. \quad (1)$$

Bloch's original work with the hydrodynamic model of the statistical atom was concerned with this problem. It is a striking feature of this average that much of the contribution in the case of heavy atoms comes from the intermediate frequencies where any detailed treatment of atomic absorption is most complicated, and where on the other hand a statistical treatment is most appropriate. The predictions of the cross section of Fig. 1 for this quantity, I , are examined at the end of this article.

2. HYDRODYNAMIC OSCILLATIONS OF THE THOMAS-FERMI ATOM

The starting point of the present analysis of the photoelectric effect at intermediate frequencies is

² A general review of stopping power is given by Fano (1963). Inokuti (1971) contains an up-to-date discussion of stopping power in the context of recent atomic physics.

³ The average rate of loss of energy per unit path via collision with electrons, excitation, and ionization in a medium containing N electrons of mass m per unit volume, by a heavy particle of velocity v and charge e is

$$-dE/dx = (4\pi N e^4 / m v^2) \{ \ln[2mv^2 / I(1 - v^2/c^2)] - (v^2/c^2) \}$$

according to Bethe (1930, 1933). The conditions for the validity of this often misquoted expression and the literature on these conditions are summarized by Wheeler and Ladenburg (1941). For a deeper treatment of the theory of stopping power see N. Bohr (1948), A. Bohr (1948), and Lindhard and Scharff (1953).

Bloch's (1933) hydrodynamic theory of the characteristic oscillations of the statistical atom model (cf. Thomas, 1926; Fermi, 1928; Gombas, 1956; March, 1951). We are not concerned with the physical reality of such atomic plasma oscillations but will consider them solely as a model for atomic excitation.⁴ Bloch treats the electrons as a degenerate Fermi gas endowed with a characteristic pressure-density relation

$$p = (\hbar^2/5m) (3/8\pi)^{2/3} n^{5/3}. \quad (2)$$

Here n is the number of electrons per unit volume. This gas is capable of existing in an equilibrium condition that is familiar from the work of Thomas and Fermi,

(potential energy of one electron)

$$V_0(\mathbf{r}) = -(Ze^2/r)\varphi(x),$$

(number density of electrons)

$$n_0(\mathbf{r}) = (32Z^2/9\pi^3) (me^2/\hbar^2)^3 [\varphi(x)/x]^{3/2}, \\ r = (\hbar^2/me^2) (9\pi^2/128Z)^{1/3} x. \quad (3)$$

The universal Thomas-Fermi function $\varphi(x)$ is that solution of the differential equation $d^2\varphi/dx^2 = \varphi^{3/2}/x^{1/2}$ which equals one at $x=0$, and for a neutral atom approaches zero as x goes to infinity. However, the gas is capable of oscillations about this steady state. Bloch introduces a velocity potential function U , which gives an irrotational flow velocity of the electron gas by the relation $\mathbf{v} = -\nabla U$. Departures from the equilibrium state are then expressed in the form

$$n(\mathbf{r}) = n_0(\mathbf{r}) + n_1(\mathbf{r}), \\ V(\mathbf{r}) = V_0(\mathbf{r}) + V_1(\mathbf{r}), \\ U(\mathbf{r}) = 0 + U_1(\mathbf{r}). \quad (4)$$

To analyze these oscillations Bloch found it sufficient to use the well-known laws of hydrodynamics together with the characteristic pressure density relation of a degenerate electron gas. The oscillating elec-

tron gas must satisfy the relations:

(Poisson's equation)

$$\nabla^2 V = -4\pi e^2 n,$$

(Continuity equation)

$$\partial n/\partial t = \nabla \cdot [n \nabla U],$$

(Newton's second law)

$$\partial U/\partial t = \frac{1}{2}(\nabla U)^2 + m^{-1} \int_0^{n(\mathbf{r})} \frac{dP(n)}{n} + \left(\frac{V}{m}\right). \quad (5)$$

Bloch neglects terms of second and higher order in the departures from equilibrium, uses the properties of the equilibrium state, and obtains linear equations for the oscillating quantities,

$$\nabla^2 V_1 = -4\pi e^2 n_1,$$

$$\partial n_1/\partial t = \nabla \cdot [n_0 \nabla U_1],$$

$$m \partial U_1/\partial t = n_1 (n^{-1} dP/dn)_{n_0} + V_1. \quad (6)$$

The gas departs from steady-state pressures and densities by an amount that can be expressed as a linear superposition of effects. Each elementary disturbance is due to a single normal mode of vibration. Any given normal mode is characterized by its frequency and by indices l and m that tell to what spherical harmonic $Y_{lm}(\theta, \varphi)$ the density and pressure variations are proportional. The amplitude of the vibrations associated with a single normal mode remains constant in time except as influenced by possible external disturbances such as the electric field of a passing particle or of a beam of radiation. In particular, the amplitude of every mode is zero for the unexcited hydrodynamic atom model. After the passage of the radiation or particle, the amplitude has increased to a finite amount. The atom has taken up energy. The amount of the uptake of a single oscillating mode provides a simple measure of a part of the stopping power or of all of the photoelectric cross section of the atom, as the case may be.

2.1. Normal Modes of Oscillation

Evidently the problem of evaluating the energy transfer falls into two distinct parts: (1) What are the characteristic modes of oscillation of the hydrodynamic atom model? (2) How much excitation does any given mode experience as a result of the external perturbation? There exists also a third question: (3) What is the relation between the hydrodynamic treatment and the machinery of standard quantum theory? This third question has been well explored for the case of a degenerate electron gas of uniform density, infinite in extent, which is neutralized by a uniform positively charged background (Nozieres and Pines, 1958; Goldstone and

⁴ The physical reality of atomic plasma oscillations, apart from their use in this paper solely as a model, has been controversial, although some collective effects undoubtedly influence the absorption spectra of atoms in the far ultraviolet and soft x-ray region. We are indebted to U. Fano for a personal memo on the history of this matter. Atomic plasma oscillations were at one time proposed to account for some features of inelastic atom-ion collisions by Afrosimov *et al.* (1964). A general discussion of these plasma oscillations, concluding against their existence, is given by Kirzhnits and Lozovik (1966). Recently an analysis of the damping of the hydrodynamic modes of oscillation of the Thomas-Fermi atom has been published by Sen and Harris (1971). A short discussion of atomic plasma oscillations from the viewpoint of microscopic quantum theory appears in Weidner and Borowitz (1966).

Gottfried, 1959).⁵ The situation is less clear with regard to atomic plasma oscillations.⁴ These questions are not central to our interest here. Instead we are concerned with obtaining definite predictions of the photoabsorption cross section from the Bloch hydrodynamic model.

Stopping power was Bloch's prime point of concern; even more specifically he focused on showing that the logarithmic mean excitation energy I [Eq. (1)] varies from atom to atom in proportion to the atomic number Z . No attempt was made at that time explicitly to integrate Eqs. (6) numerically to determine the constant of proportionality in the formula $I \propto Z$. Still less was any attempt made to give a general expression for the photoabsorption cross section or to calculate it. Moreover, the very existence of a curve for photoabsorption cross section as a function of frequency implies a continuous distribution of characteristic frequencies. In contrast, at the time Bloch carried out his pioneering analysis the spectrum of characteristic frequencies of the statistical atom was envisaged as discrete.

Only an explicit analysis of the boundary conditions permits one to say whether the spectrum is discrete or continuous. To carry out this analysis is an essential first part of the present work. It leads to the conclusion that the spectrum for a neutral atom is continuous (contrary to the tacit assumptions of early work).

That the spectrum for the neutral atom is continuous is only revealed by a detailed examination of the amplitudes of the normal modes of oscillation at large distances. Were these amplitudes to go to zero sufficiently rapidly with increasing r , the disturbance would be confined to what is effectively a finite volume, as in the case of an ion [where the Thomas-Fermi function $\varphi(x)$ vanishes at a finite x value], and the spectrum would be discrete. Quite in contrast to this conceivable outcome is the actual situation for the neutral Thomas-Fermi atom, for which at large distances the Thomas-Fermi function decreases as x^{-3} . In these conditions we find (Appendix A) the asymptotic form of the radial part of the disturbances in number density of electrons and velocity potential and potential energy per electron,

$$\begin{aligned} n_1(\Omega, x) &\sim x^{-1} \sin [\text{const} + \int^x (\sqrt{3}\pi\Omega x^2 dx/2^6)], \\ U_1(\Omega, x) &\sim x \sin [\text{const} + \int^x (\sqrt{3}\pi\Omega x^2 dx/2^6)], \\ V_1(\Omega, x) &\sim -\Omega^{-2}x^{-5} \sin [\text{const} + \int^x (\sqrt{3}\pi\Omega x^2 dx/2^6)]. \end{aligned} \quad (7)$$

Here Ω is the quantum energy $\hbar\omega$ in units of Z times 27.2 eV, and x is the Thomas-Fermi distance parameter of Eq. (3). The problem of hydrodynamic oscillation may be formulated entirely in terms of these two

dimensionless parameters. Calculations done in terms of these parameters scale in a simple way with the atomic number Z and thus may be applied to all atoms.

The unperturbed electron density of the neutral Thomas-Fermi atom behaves asymptotically as x^{-6} . Consequently at large distances the perturbation of the number density becomes larger than the number density itself. Clearly at these large distances the linear approximation is of doubtful applicability. The validity of the linear approximation is a physical question of importance if the physical results depend upon the behavior of the normal mode functions at large distances. Such is not the case for the intermediate frequency regime in which we are primarily interested. As discussed below, the photoabsorption cross section is largely determined by the behavior of the normal mode function in the vicinity of its principal (first) maximum. At intermediate frequencies the principal maximum falls at intermediate radial distances. We therefore focus attention upon the well-defined mathematical problem of the frequency spectrum of normal modes of the linear equations.

We first replace the boundary at infinity by an artificial grounded spherical boundary at a large radial distance. The requirement that both the potential energy per electron and the normal flow velocity vanish at this boundary determines the boundary conditions:

$$\begin{aligned} V_1(\Omega, x) |_{\text{bound}} &= 0, \\ dU_1(\Omega, x)/dx |_{\text{bound}} &= 0. \end{aligned} \quad (8)$$

These boundary conditions can be satisfied if the phase of the sine function of Eq. (7) has a certain specific value, δ —a value which it is unnecessary to calculate—or this value plus any integral multiple of π ; thus,

$$\text{const} + \pi\Omega 3^{-1/2} 2^{-6} x_{\text{bound}}^3 = \delta + N\pi.$$

This eigenvalue condition immediately determines the density of characteristic frequencies,

$$dN/d\Omega = 3^{-1/2} 2^{-6} x_{\text{bound}}^3. \quad (9)$$

When the boundary is moved to infinity, to correspond to the actual case of the neutral Thomas-Fermi atom, the eigenvalue spectrum evidently becomes continuous.

If one takes the normal modes of oscillation to be of the form

$$\begin{aligned} n_1 &= -\omega N_{\omega lm}(\mathbf{r}) \sin(\omega t + \delta) \\ U_1 &= U_{\omega lm}(\mathbf{r}) \cos(\omega t + \delta) \\ V_1 &= m\omega V_{\omega lm}(\mathbf{r}) \sin(\omega t + \delta), \end{aligned} \quad (10)$$

then by Eq. (6) the spatial parts of the normal modes are the solutions of the set of coupled equations:

$$\begin{aligned} \nabla^2 V_{\omega lm} &= (4\pi e^2/m) N_{\omega lm} \\ -\omega^2 N_{\omega lm} &= \nabla \cdot (n_0 \nabla U_{\omega lm}) \\ -U_{\omega lm} &= -N_{\omega lm} (m^{-1} n^{-1} dP/dn)_{n_0} + V_{\omega lm}. \end{aligned} \quad (11)$$

⁵ Plasma oscillations in an inhomogeneous plasma, particularly near a fixed charge singularity, are examined in Sziklas (1965).

These equations we shall solve later by the method of separation of variables followed by numerical integration. The set of three coupled equations immediately reduces to a set of two second-order equations coupling the normal mode of the number density and the normal mode of the velocity potential. Bloch was able to show that the normal mode functions exhibit an orthogonality property, a feature which facilitates the calculation of the photoabsorption. The functions $N_{\omega lm}$ and $U_{\omega lm}$ are not the Hermitian conjugates one to the other; rather, one is said to be "dual" to the other. Moreover the functions $N_{\omega lm}$ are not orthogonal among themselves, nor are the functions $U_{\omega lm}$ orthogonal among themselves. Rather the functions $N_{\omega lm}$ and $U_{\omega' l' m'}$ are biorthogonal, in the sense that the product of the two kinds of functions has to be taken and integrated over volume to give any meaningful scalar product. This scalar product automatically vanishes when the two functions have different spherical harmonic indices l and m . In addition, the radial boundary conditions suffice to show biorthogonality when frequency indices differ; thus,

$$\int U_{lm}(\omega, \mathbf{r}) N_{l'm'}(\omega', \mathbf{r}) d\tau = k \delta_{ll'} \delta_{mm'} \delta(\omega - \omega'). \quad (12)$$

The integration goes over the entire volume of the atom. Here we have written the frequency as a continuous index to reflect the continuous spectrum of eigenfrequencies. The constant k is fixed by the density of characteristic frequencies and by the normalization of the functions,

$$k^{-1} = \lim_{r_{\text{bound}} \rightarrow \infty} (dN/d\omega) / \int N_{lm}(\omega, \mathbf{r}) U_{lm}(\omega, \mathbf{r}) d\tau. \quad (13)$$

The normalization of the functions $N_{lm}(\omega, \mathbf{r})$ and $U_{lm}(\omega, \mathbf{r})$ is determined by their asymptotic behavior, Eq. (7). Both numerator and denominator in the expression for k increase as r_{bound}^3 , resulting in a finite value for k . Biorthogonality expresses the linear independence of normal modes of different frequency and angular dependence. In the following we make the additional assumption of completeness, which together with biorthogonality, allows any well-behaved function to be expanded in terms of either the normal modes of number density or of the normal modes of velocity potential.

2.2. Oscillation Energy and the Photoabsorption Cross Section

The energy of the oscillating atom is described in terms of the amplitudes of its normal modes of free oscillation. The total energy of the hydrodynamic atom is the sum of three parts: (1) the kinetic energy of the average flow velocity, (2) the electrostatic potential energy, and (3) the pressure energy, which is really the kinetic energy of electrons in the degenerate Fermi

gas; thus,

$$E = \frac{1}{2} \int nm(\nabla U)^2 d\tau + \frac{1}{2} \int nV d\tau + \int d\tau n \int_0^n [p(n^*)/n^{*2}] dn^*.$$

This relation is expanded to second order in the departures from equilibrium, n_1 , V_1 , and U_1 of Eq. (4). The zeroth-order terms furnish the energy of the static Thomas-Fermi atom. The sum of terms linear in the departures from equilibrium vanishes, as it must, since we expand about the equilibrium state. The second-order terms represent the additional energy of hydrodynamic oscillation. The boundary conditions, the equations of motion, and the pressure-density relation enable the energy of hydrodynamic oscillation to be recast into a convenient form,

$$E_2 = \frac{1}{2} m \int d\tau [n_1(\partial U_1/\partial t) - U_1(\partial n_1/\partial t)]. \quad (14)$$

A general state of free oscillation of the atom is a superposition of the normal modes of Eq. (10) with amplitudes $c_{lm}(\omega)$. The biorthogonality of the normal modes (with number density dual to velocity potential) insures that each normal mode contributes independently to the energy. Consequently the total energy of free oscillation can be written

$$E_2 = \frac{1}{2} m k \sum_{lm} \int \omega^2 c_{lm}^2(\omega) d\omega, \quad (15)$$

a result which is independent of time.

In order to calculate the photoabsorption cross section one must consider the manner in which the normal modes are excited by the electric field of a plane wave. For wavelengths of radiation large in comparison to atomic size the potential energy per electron of a plane wave polarized in the z direction is

$$V_p = ez\mathcal{E} \sin \omega_0 t,$$

where \mathcal{E} is the constant electric field amplitude of the plane wave. This additional potential energy must be introduced into the equations of motion, Eqs. (6), of the oscillating quantities, it enters the third equation but not the first, since its Laplacian is zero. The perturbing potential has dipole symmetry and only excites modes of angular dependence $\cos \theta$ ($m=0, l=1$). Moreover it is clear that the perturbing forces are irrotational, which justifies the use of a scalar velocity potential. We seek as a solution for the response of the atom a superposition of normal modes of this symmetry

with time-dependent coefficients,

$$\begin{aligned} n_1 &= \int_0^\infty g_{10}(\omega, t) N_{10}(\omega, \mathbf{r}) d\omega, \\ U_1 &= \int_0^\infty h_{10}(\omega, t) U_{10}(\omega, \mathbf{r}) d\omega, \\ V_1 &= \int_0^\infty l_{10}(\omega, t) V_{10}(\omega, \mathbf{r}) d\omega. \end{aligned} \quad (16)$$

In addition it is convenient to employ the biorthogonality relation to expand the spatial part of V_p in terms of normal modes of velocity potential,

$$V_p = \sin \omega_0 t \int_0^\infty v_{10}(\omega) U_{10}(\omega, \mathbf{r}) d\omega. \quad (17)$$

The expansion coefficient, a function of frequency alone, is then given by the relation

$$v_{10}(\omega) = (e\mathcal{E}/k) \int z N_{10}(\omega, \mathbf{r}) d\tau. \quad (18)$$

Substitution of Eqs. (16) and (17) into the equations of motion [Eqs. (6)] results in equations of motion for the time-dependent coefficients. One finds $l_{10} = -mg_{10}$, $g_{10} = -\omega^2 h_{10}$ and

$$\ddot{g}_{10}(\omega, t) + \omega^2 g_{10}(\omega, t) = -(\omega^2/m) v_{10}(\omega) \sin \omega_0 t. \quad (19)$$

The amplitude of each normal mode responds as an harmonic oscillator driven by an oscillating function of frequency ω_0 . The strength of the driving function is determined by the function $v_{10}(\omega)$, an integral proportional to the dipole moment of the spatial distribution of charge in the mode. The entire coupling of the hydrodynamic atom with the radiation field of a plane wave is embodied in this integral. We now imagine the potential of the plane wave to be switched on at $t=0$ and then switched off after a time t large in comparison to the period of the plane wave. Initially the amplitude of the normal modes of both velocity potential and number density is zero. These initial conditions require the solution of Eq. (19) to be

$$g_{10}(\omega, t) = \frac{v_{10}(\omega)}{m} \frac{\omega_0 \omega \sin \omega t - \omega^2 \sin \omega_0 t}{\omega^2 - \omega_0^2}. \quad (20)$$

After the potential is switched off the state of the atom will be given by a superposition of free oscillations. The amplitude of free oscillation at time t and subsequently is determined by comparison of Eq. (20) with Eqs. (10), with the result,

$$\omega^2 c_{10}^2(\omega) = g_{10}^2(\omega, t) + \dot{g}_{10}^2(\omega, t) / \omega^2.$$

The total energy which the atom has absorbed at a time t is given by the integral of Eq. (15), an integral over all frequencies. The resonance behavior of the integrand has the consequence that at large times essentially all the absorbed energy has gone into the resonant

normal mode. At time t the model atom has absorbed an energy,

$$E_2(t) = (\pi k/4m) v_{10}^2(\omega_0) \omega_0^2 [t - (\sin 2\omega_0 t / 2\omega_0)].$$

For times large compared to the period of the disturbance the oscillating second term may be neglected in comparison with the term that increases linearly with time. The average rate at which energy is absorbed is a constant. The rate of energy absorption divided by the energy flux of the incident plane wave, $c\mathcal{E}^2/8\pi$, gives the atomic photoabsorption cross section as a function of frequency,

$$\sigma(\omega) = (2\pi^2 e^2/mc) (\omega^2/k) [\int z N_{10}(\omega, \mathbf{r}) d\tau]^2. \quad (21)$$

This equation is the basis of our calculation of the atomic photoabsorption cross section, Fig. 1, predicted by the Bloch model of the oscillating Thomas-Fermi atom. As suggested above, and as one might anticipate upon physical grounds, the dipole integral (the quantity in square brackets) determines the cross section. This dipole integral is evidently the analog in the classical hydrodynamic theory of the dipole matrix element of standard quantum theory.

The form of Eq. (21) is not an exact analog of the expression for the photoabsorption cross section in standard quantum theory given, for example, by Eq. (2.3) of Fano and Cooper (1968),

$$\sigma(\omega) = (\text{const}) \omega | \langle \omega | z | 0 \rangle |^2.$$

However, it would be possible to alter the analysis somewhat and exhibit a much closer analogy. There are two points here: (1) the fluctuation in number density of electrons in a normal mode is not $N_{\omega_{10}}$ but rather by Eq. (10) $\omega N_{\omega_{10}}$. Consequently the factor of ω^2 in Eq. (21) could be included in the square of the dipole integral in order to obtain a quantity analogous to the square of the dipole matrix element of standard quantum theory; (2) The additional factor of ω present in the quantum formula outside the square of the matrix element is absent in Eq. (21). This feature results from our choice of a frequency-independent normalization for the normal mode functions. The normalization is fixed by the amplitudes of these oscillating functions at large radial distances given by Eq. (A7). One could choose these amplitudes to include an additional factor of $\omega^{-1/2}$, which perhaps would be more conventional for a JWKB asymptotic approximation. In this case the constant k^{-1} would be proportional to the frequency ω . With these two changes Eq. (21) would assume a form closely analogous to the quantum expression.

3. NUMERICAL CALCULATIONS AND RESULTS ON THE HYDRODYNAMIC MODEL

To evaluate the cross section requires knowledge of the normal modes of free oscillation, quantities which

are solutions of the coupled equations of motion, Eqs. (11.) Although these equations are linear they depend upon the charge distribution of the neutral Thomas-Fermi atom for which there is no analytic form which is both simple and accurate at all radial distance. Therefore the solutions must be computed numerically. Appendix A presents the procedure used in our numerical calculation of the normal mode functions. We note here, however, that the calculation contains some unusual features. The two boundary conditions of Eq. (8) are not sufficient to determine a unique solution of the two coupled second-order equations, which possess four linearly independent solutions. A linear combination of the four solutions must be chosen which satisfies the boundary conditions at large distances and which also gives physically reasonable behavior at the origin. The desired solutions start at $r=0$ with zero tangent, rise quasiexponentially to a first maximum, and then start oscillating more and more rapidly, eventually approaching the asymptotic behavior of Eqs. (7). Our calculation continues these rapid oscillations by a JWKB approximation which provides an accurate extension of the numerical solutions into the region of rapid oscillation. The equations possess one solution which increases without limit at large distances, an unstable solution which always appears in the numerical computation owing to small errors in the step-by-step integration. Only by following the solution into the asymptotic region is one able to choose the linear combination which eliminates the unstable solution and which fully satisfies the boundary conditions both at the origin and at large distances.

The details of the numerical calculation of the dipole integral are given in Appendix B. These calculations do not evaluate the dipole integral directly from the normal mode of number density. To do so is inconvenient because (a) at large radial distances the integrand increases in amplitude and oscillates more and more rapidly and (b) the boundary conditions require that the integration be stopped at a definite phase of the oscillating function—a condition difficult to apply. We use the equation of continuity and also the boundary conditions to re-express the dipole integral by an equivalent expression written in terms of the normal mode of velocity potential. For modes of dipole symmetry the relation is

$$\int z N_{10}(\omega, \mathbf{r}) d\tau = \omega^{-2} \int \cos \theta U_{10}(\omega, \mathbf{r}) (dn_0/dr) d\tau. \quad (22)$$

The integral over the velocity potential is convenient for numerical evaluation since the presence of the number density gradient for the neutral atom causes the amplitude of the oscillating integrand to diminish rapidly with distance. This behavior is illustrated in Fig. 6 where a quantity proportional to this integrand is plotted.

The rapid oscillations of the normal mode functions

have the consequence that there is little contribution to the dipole integral from distances larger than the vicinity of the first maximum. At extremely low frequencies the first maximum is at large radial distance and it moves inward as the frequency increases. This behavior conforms with the rough qualitative idea that the principal maximum is located at that radial distance for which the local plasma frequency (given by the electron number density n_0) is the same as the frequency of the mode. At very high frequencies the first maximum is very near the nucleus. For neither extremely low frequencies nor extremely high frequencies can the hydrodynamic model be expected to give good results. In both regions, near the nucleus and far from it, the Thomas-Fermi statistical atom gives grossly unrealistic electron charge densities. Moreover, for physical reasons cited earlier, one does not expect reliable predictions from the Bloch hydrodynamic model at these extremes of frequency. However the Bloch model does furnish good results for the photo-absorption cross section at the intermediate frequencies in which we are interested. At these frequencies the cross section depends upon the behavior of the normal

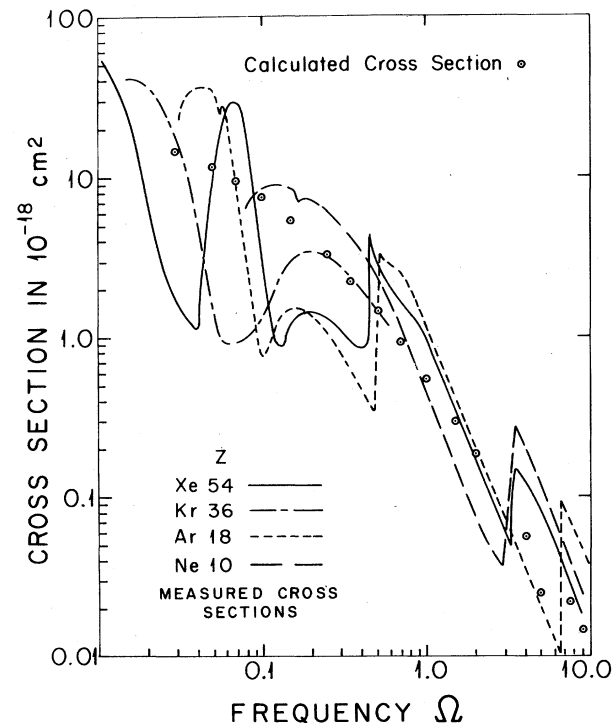


FIG. 2. A comparison of the calculated universal atomic photo-absorption cross section of Fig. 1 with experimentally measured cross sections of the noble gases. The smooth curves average the measured values tabulated in the review article of Samson (1966) and also given by Fano and Cooper (1968). The experimental cross sections are plotted as a function of the frequency parameter $\Omega = (\text{photon energy in eV}) / (27.2Z \text{ eV})$. Consequently a given value of Ω corresponds to different photon energies for elements of different atomic number Z .

mode functions at intermediate radial distances, a range in which the Thomas-Fermi model provides a realistic number density of electrons.

3.1. Comparison with Experiment

In Fig. 2 our calculated photoabsorption cross section for the intermediate frequency region is compared with some experimental cross sections of the noble gases. These elements are the only ones for which reasonably complete data exist at the frequencies of interest. We have used the experimental measurements reported in review articles by Samson (1966) and by Fano and Cooper (1968). The experimental data for each element are plotted as a smooth curve which approximately averages the experimental points and omits narrow resonances and windows. All cross sections are plotted as a function of the dimensionless frequency Ω . Recall that $\omega = \text{const}Z\Omega$. Thus a particular value of the abscissa corresponds to different values of the photon frequency according to which element is considered. The experimental cross sections exhibit a great deal of structure which is not present in the smooth curve of the cross section computed from the Bloch model. The peaks and absorption edges of the experimental cross sections are a consequence of the atomic shell structure which is ignored in the Thomas-Fermi model. The hydrodynamic model based upon the Thomas-Fermi atom does, however, give a good estimate of the absorption cross section of heavy atoms which is certainly within an order of magnitude even in the neighborhood of absorption edges. At low frequencies $\Omega < 0.1$ the agreement of the hydrodynamic model is more doubtful. There the experimental cross sections fluctuate widely, but more important, the calculated cross section seems too high to be a proper average of the experimental cross sections. This situation can be traced to an overestimate of electron densities at large distances by the Thomas-Fermi model of the neutral atom, contrasted with the actual rapid decrease of electron density near the atomic boundary of noble gases. For example, the hydrodynamic cross section at $\Omega = 0.1$ is largely determined by electron densities at a radial distance of $x \approx 6$. At this distance the Thomas-Fermi model already gives an electron density for argon which exceeds the electron density given by Hartree-Fock calculations (Gombas, 1956). This shortcoming of the hydrodynamic cross sections—based upon the neutral Thomas-Fermi atom—at low frequencies is brought out more clearly below in the calculation of the logarithmic mean excitation energy.

3.2. Oscillator Strengths and Sum Rule

Sometimes one is less interested in the cross section itself than in the number of equivalent harmonic oscillators, df , to which one can ascribe the absorption that

occurs in a given range of circular frequency, $d\omega$. The two quantities are connected by the relation (Breit and Korff, 1932)⁶

$$\sigma = (2\pi^2 e^2 / mc) (df / d\omega).$$

Comparing this with our expression for the cross section we see that the hydrodynamic model predicts a distribution of oscillator strength,

$$df = (\omega^2 / k) [\int z N_{10}(\omega, \mathbf{r}) d\tau]^2 d\omega.$$

The integrated oscillator strength must obey the dipole sum rule of Kuhn-Reiche-Thomas and equal the total number of atomic electrons Z . The completeness property of the biorthogonal set of functions $N_{\omega lm}$ and $U_{\omega lm}$ can be used to show that the oscillator strengths predicted by the Bloch hydrodynamic model do indeed satisfy the sum rule. The square of the dipole integral may be written as the product of the two equivalent expressions given by Eq. (22). One of these equivalent factors is the coefficient in the expansion of z in terms of the functions $U_{\omega 10}$; the other is the coefficient in the expansion of $\cos \theta dn_0/dr$ in terms of the functions $N_{\omega 10}$; i.e.,

$$a(\omega) = k^{-1} \int z N_{\omega 10} d\tau;$$

$$z = \int a(\omega) U_{\omega 10} d\omega;$$

$$b(\omega) = k^{-1} \int \cos \theta (dn_0/dr) U_{\omega 10} d\tau;$$

$$\cos \theta dn_0/dr = \int b(\omega) N_{\omega 10} d\omega.$$

Therefore the integrated oscillator strength takes the form

$$\int df = -k \int a(\omega) b(\omega) d\omega.$$

By the completeness relation, the analog in our formalism of the Parseval relation of Fourier analysis, this integral over frequency of the product of the two expansion coefficients equals the integral over the atomic volume of the product of the two functions which are expanded

$$\int df = - \int z \cos \theta (dn_0/dr) d\tau = Z.$$

An integration by parts reduces the volume integral to an integral over volume of the number density of electrons in the Thomas-Fermi atom at equilibrium, thus verifying the sum rule.

3.3. Limits of Cross Section at Extremes of Frequency

At very high frequencies and at very low frequencies simplifying features are present which enable the photoabsorption cross section to be calculated analytically. These calculations, which are presented in Appendix B, give asymptotic estimates of the cross section at very

⁶ See also Eq. (2.3) and discussion in Fano and Cooper (1968).

high and at very low frequencies

$$\begin{aligned} \sigma(\Omega) &\sim [1.24(10)^{-18} \text{ cm}^2]/\Omega^2, & \Omega > 10, \\ \sigma(\Omega) &\sim 207.5(10)^{-18} \text{ cm}^2, & \Omega < 3(10)^{-5}. \end{aligned} \quad (23)$$

Again Ω is the frequency parameter previously introduced. The photoabsorption cross section approaches a constant at zero frequency and at high frequencies decreases as the inverse square of the frequency. Although neither of these limiting results can be expected to apply to the real physical problem, they are useful to round out and complete the analysis of what the oscillating Thomas-Fermi atom predicts for the photoabsorption cross section. In particular these limiting forms permit calculation of two quantities which depend upon the integral of the cross section over all frequencies: (1) the sum rule for total oscillator strength, and (2) the logarithmic mean excitation energy of Eq. (1).

3.4. Check of Sum Rule

In terms of the parameter Ω the sum rule predicts an integrated cross section,

$$\int_0^\infty \sigma(\Omega) d\Omega = 2\pi^2 (e^2/\hbar c) (\hbar^2/me^2)^2 = 4.02(10)^{-18} \text{ cm}^2. \quad (24)$$

We explicitly evaluated the same quantity using for the cross sections:

Range of Ω	Cross section in cm^2
$0 < \Omega < 3(10)^{-5}$	$207.5(10)^{-18}$ (low-freq. limit)
$3(10)^{-5} < \Omega < 0.03$	$3.84(10)^{-18}/\Omega^{0.383}$ (interpolation)
$0.03 < \Omega < 10.0$	Values of Table I (numerically computed)
$10.0 < \Omega < \infty$	$1.24(10)^{-18}/\Omega^2$ (high-freq. limit).

The result is

$$\int \sigma(\Omega) d\Omega = 3.95(10)^{-18} \text{ cm}^2, \quad (25)$$

which checks the theoretical sum rule to within 2%. Approximately 80% of the contribution to the integral comes from the intermediate frequency range where numerical values of the cross section were computed and within which the hydrodynamic model is most accurate.

3.5. The Logarithmic Mean Excitation Energy

The mean excitation energy of Eq. (1), written in terms of the parameter Ω , is

$$\ln I = \ln (Zme^4/\hbar^2) + \left[\int_0^\infty \sigma(\Omega) \ln \Omega d\Omega / \int_0^\infty \sigma(\Omega) d\Omega \right]. \quad (26)$$

Divide the cross section $\sigma(\Omega)$ in the numerator by the integrated cross section in the denominator (integral known from the sum rule). Multiply by $\ln \Omega$ and integrate over Ω , with the following contributions:

Ω from 0 to 0.03	-0.924
Ω from 0.03 to 10	-0.884
Ω from 10 to ∞	+0.102
Total	-1.706

$$\text{Resultant } \ln I = \ln (Zme^4/\hbar^2) + \ln [-1.706]$$

$$\text{Resultant } I = 0.182Zme^4/\hbar^2 = 4.95Z \text{ eV}. \quad (27)$$

The proportionality of the logarithmic mean excitation energy to the atomic number was one of the most important results obtained by Bloch in his original work and follows directly out of the scaling properties of the Thomas-Fermi statistical atom. The new result of the present calculation is the constant of proportionality, 4.95Z eV. This result is too low by a factor of ~ 2 to accord at all with observation. It is true that experimental values of I based upon an unsophisticated application of an over-simple stopping power formula (no correction for the inability of a slow moving charged particle to excite deeply bound electrons) sometimes gives values as low as 8.0 eV at low energies and 16.0 eV at high energies. However, when corrections are made for these and other effects the constant of proportionality I/Z as determined experimentally is found to lie in the range 9.5 to 16.0 eV,⁷ twice as high as the calculated value. The reason is not far to seek. The universal photoabsorption curve is being used outside its range of validity. It is (falsely) making a very large contribution to $(\ln \omega)_{av}$ in the range of low frequencies (outermost several electrons) where a statistical picture is completely inappropriate. The direction of the error is clear and two features of the statistical atom contribute to it. First, the electron distribution of the simple Thomas-Fermi atom model falls to 1/100 of the central density at values of r much larger than those for the real atom. In consequence the number of electrons that absorb at low frequencies is wildly overestimated. This feature is already apparent at values of $\Omega \approx 0.05$, as can be seen in Fig. 2, where the universal photoabsorption cross section is compared with measured cross sections of the noble gases. Second, the hydrodynamic model of the neutral atom puts all the oscillator strength in the continuum and extends the continuum down to zero frequency. By contrast, real atoms have a lowest excitation energy and the continuum starts at the first ionization energy.

No simple modification of the calculation corrects these difficulties. Take Xe ($Z=54$) as an example. The

⁷ See, for example, Fano (1963).

lowest excitation lies at 8.4 eV. There is zero electron number to be assigned to the photoabsorption cross section below this point [$\Omega=8.4$ eV/54(27.2 eV) = 0.00572]. The universal photoabsorption curve (as interpolated between the numerically computed points and the analytically computed point at $\Omega=0$) gives for the electron number in this region

$$f = Z \int_0^{0.00572} \sigma(\Omega) d\Omega / \int_0^\infty \sigma(\Omega) d\Omega = 3.38.$$

If we take these 3.38 effective electrons whose absorption is so unrealistically treated and move all their absorption, for example, to a single "line" located at the first ionization potential of Xe, 12.1 eV, leave all the rest of the "universal photoabsorption curve" unchanged, and recompute the logarithmic mean excitation energy as given by the new distribution of absorption, we find

$$I/Z = 5.69 \text{ eV.} \quad (28)$$

This calculation corrects the logarithmic mean absorption energy in the right direction, but not nearly enough to agree with experimental measurements. Evidently the Bloch model predicts a photoabsorption cross section which is too large not only at very low frequencies ($\Omega < 0.01$) but also at somewhat higher frequencies ($0.01 < \Omega < 0.1$).

The fact that the universal photoabsorption curve does not apply at these low frequencies in no way impairs its usefulness for estimating the contribution to the logarithmic mean excitation energy at higher frequencies where it is approximately correct. One may use the photoabsorption curve for frequencies greater than $\Omega=0.03$, provided the cross section below this frequency can be obtained by other means (either measurement or calculation). We separate the contribution to the logarithmic mean excitation energy into these two parts and obtain

$$\ln I = \ln(Zme^4/\hbar^2) + \beta - 0.782.$$

Here the number,

$$-0.782 = \int_{0.03}^\infty \sigma(\Omega) \ln \Omega d\Omega / \int_0^\infty \sigma(\Omega) d\Omega,$$

is provided by the universal photoabsorption curve. The parameter β depends upon the absorption cross section below $\Omega=0.03$ and is given by

$$\beta = \int_0^{0.03} \sigma(\Omega) \ln \Omega d\Omega / \int_0^\infty \sigma(\Omega) d\Omega.$$

If experimental values of the cross section are used to evaluate β , the scaling introduces a dependence upon the atomic number. Thus β is a negative parameter which varies from atom to atom and takes into account the behavior of valence electrons. This separation incorporates all that the Bloch model can realistically

say about the logarithmic mean excitation energy and provides the formula

$$I = 12.4e^\beta Z \text{ eV,} \quad (29)$$

where the negative parameter β takes into account the oscillator strength at low frequencies. The proportionality of I to the atomic number is only approximate and is true only insofar as the logarithmic mean excitation energy depends upon the excitation at intermediate and high frequencies.

4. CONCLUSION

In summary, the Bloch hydrodynamic model of the Thomas-Fermi atom provides a reasonable model for atomic excitation which, although approximate, nevertheless gives a reasonable estimate of the atomic photoabsorption cross section at intermediate frequencies. In this frequency region ($0.03 < \Omega < 10.0$) which for heavy atoms ranges from the ultraviolet to the soft x-ray region, the Bloch model does as well as could be expected in providing a global photoabsorption curve, applicable to all atoms. The classical concept of atomic hydrodynamic oscillation is undoubtedly a limiting factor in the applicability of this model, but a more severe limitation appears to arise from the defects of the statistical Thomas-Fermi atom itself. This situation becomes especially clear at low frequencies where the inaccuracies of the hydrodynamic photoabsorption cross section are directly traceable to the exaggeration of electronic charge densities at large radial distance by the Thomas-Fermi model.

None the less the conceptual simplicity of the Bloch hydrodynamic model is attractive and it offers an approach which probably has never been properly exploited. Numerical computations based upon it furnish fair approximations. Although up to now its use has been limited to the photoabsorption problem treated here, there exists the possibility that it could be applied to other atomic processes for which standard methods are unable to yield useful results.

ACKNOWLEDGMENTS

One of the authors (JAB) wishes to thank the physics departments of Bryn Mawr College and of Montana State University for the use of their facilities and for providing drafting and clerical assistance. We also wish to express our gratitude to the staff of the computing center at the Courant Institute of Mathematical Sciences for their courteous assistance with the numerical calculations.

APPENDIX A: NUMERICAL SOLUTION OF THE COUPLED HYDRODYNAMIC EQUATIONS

Before proceeding to an analysis of the solutions of the coupled hydrodynamic equations, it is convenient

to express both the dependent and independent variables in terms of dimensionless quantities appropriate to the neutral Thomas–Fermi atom. Thereby one not only eliminates physical constants from the pure mathematical analysis, but also obtains results which are applicable to atoms of all atomic numbers Z by a simple change of scale. The radial distance r and the circular frequency ω are expressed in terms of the parameters x and Ω , respectively,

$$\begin{aligned} r &= (\hbar^2/me^2) (9\pi^2/128Z)^{1/3} x, \\ \omega &= (me^4/\hbar^3) Z\Omega. \end{aligned} \quad (\text{A1})$$

Similarly the equilibrium number density of electrons in the neutral Thomas–Fermi atom is written in terms of the universal Thomas–Fermi function $\varphi(x)$

$$n_0(x) = (32Z^2/9\pi^3) (me^2/\hbar^2)^3 (\varphi/x)^{3/2}. \quad (3)$$

With these substitutions the normal mode functions can be expressed in terms of two new dimensionless radial functions: $G_l(\Omega, x)$ the velocity potential factor, and $H_l(\Omega, x)$ the potential energy factor;

$$N_l(\Omega, \mathbf{x}) = \frac{m^2 e^2}{\hbar^3} \left(\frac{2^5 Z^2}{3\pi^7} \right)^{1/3} \left[\frac{G}{(x^3 \varphi)^{1/4}} + \frac{\varphi^{1/2} H}{x^{3/2}} \right] P_l(\cos \theta),$$

$$U_l(\Omega, \mathbf{x}) = (\hbar/m) [G/(x\varphi^3)^{1/4}] P_l(\cos \theta),$$

$$V_l(\Omega, \mathbf{x}) = (\hbar/m) (H/x) P_l(\cos \theta). \quad (\text{A2})$$

The particular forms of Eqs. (A2) are chosen to eliminate the first derivative term from the coupled equations, a feature which greatly facilitates the analysis. Substitution of Eqs. (A2) into the coupled equations for normal modes, Eqs. (11), gives a set of coupled equations for H and G in which the first derivatives are absent; i.e.,

$$\begin{aligned} G'' &= (GG)G + (GH)H \\ H'' &= (HG)G + (HH)H. \end{aligned} \quad (\text{A3})$$

The coefficients in this equation are

$$\begin{aligned} (GG) &= [l(l+1) - 3/16] x^{-2} \\ &+ \frac{3}{8x} \left(\frac{\varphi'}{\varphi} \right) - \frac{3}{16} \left(\frac{\varphi'}{\varphi} \right)^2 + \frac{3}{4} \left(\frac{\varphi'}{x} \right)^{1/2} - \frac{27\pi^2 \Omega^2 x}{256 \varphi}, \end{aligned}$$

$$(GH) = -(27\pi^2 \Omega^2 / 256) (x/\varphi)^{1/4},$$

$$(HG) = \frac{3}{2} (x/\varphi)^{1/4},$$

$$(HH) = [l(l+1)/x^2] + \frac{3}{2} (\varphi/x)^{1/2}. \quad (\text{A4})$$

The boundary conditions, Eq. (8), furnish the boundary conditions of G and H ,

$$\begin{aligned} (d/dx)[G/(x\varphi^3)^{1/4}]_{\text{bound}} &= 0, \\ [H/x]_{\text{bound}} &= 0. \end{aligned} \quad (\text{A5})$$

Asymptotic Forms of G and H

At large radial distances, $x > 100$, the asymptotic form of the Thomas–Fermi function $\varphi = 144/x^3$ may

be used. This substitution, in which only the dominant terms in the coefficients are retained, leads to a form of the coupled equations which is asymptotically valid at large distances,

$$\begin{aligned} G'' &= -(3\pi^2 \Omega^2 x^4 / 4^6) G - (3^{5/4} \pi^2 \Omega^2 x / 2^9) H, \\ H'' &= (3^{1/2} x / 4) G + (20/x^2) H. \end{aligned} \quad (\text{A6})$$

We expect a solution which is a linear combination of four independent solutions. Let us first assume that the function G is dominant: G drives H but H does not drive G . This assumption seems justified by the relative magnitude of the coefficients at large distances. Under these conditions the JWKB analysis gives for G ,

$$G_{12} = (2^3 / 3^{1/4} \pi^{1/2} x) \sin [\text{const} + \int^x (\sqrt{3} \pi \Omega x^2 / 2^6) dx],$$

with the corresponding solution for H ,

$$H_{12} = (-2^{13} / 3^{3/4} \pi^{5/2} \Omega^2 x^4) \sin [\text{const} + \int^x (\sqrt{3} \pi \Omega x^2 / 2^6) dx].$$

These are two independent solutions since the sine and the cosine are both equally acceptable.

To obtain two other independent solutions we assume that H is dominant. This implies that in spite of the relatively small magnitudes of (GH) and (HH) in the asymptotic region, H is large enough to drive G and G is so small that it does not drive H . These conditions give the two solutions,

$$H_3 = x^{(1/2)+(1/2)[1+4(l^2+l+18)]^{1/2}},$$

$$G_3 = -3^{3/2} 2^3 x^{-(5/2)+(1/2)[1+4(l^2+l+18)]^{1/2}},$$

$$H_4 = x^{(1/2)-(1/2)[1+4(l^2+l+18)]^{1/2}},$$

$$G_4 = -3^{3/2} 2^3 x^{-(5/2)-(1/2)[1+4(l^2+l+18)]^{1/2}}.$$

Solution three must be excluded since H_3 increases at large distances in such a way that the boundary condition on the potential can never be satisfied. The solutions H_1 , H_2 , and H_4 are acceptable since they do satisfy the boundary condition when the boundary surface moves to infinity. Therefore, at large distances the asymptotic solution G is also a linear combination of the three solutions G_1 , G_2 , and G_4 . The oscillating solutions for G decrease more slowly than any of the other solutions. We establish a canonical normalization for the functions G and H by requiring that at large radial distance G and H approach the normalized asymptotic form,

$$\begin{aligned} G_N &= (2^3 / 3^{1/4} \pi^{1/2} x) \sin [\text{const} + (\pi \Omega x^3 / \sqrt{3} 2^6)], \\ H_N &= (-2^{13} / 3^{3/4} \pi^{5/2} \Omega^2 x^4) \sin [\text{const} + (\pi \Omega x^3 / \sqrt{3} 2^6)], \end{aligned} \quad (\text{A7})$$

which is independent of the angular index l . These canonically normalized functions G_N and H_N determine the asymptotic behavior of the physical normal modes of number density, velocity potential, and potential energy per electron which are given by Eq. (7). In the limit as the boundary moves to infinity the

boundary condition on H of Eq. (A5) is automatically satisfied. However the boundary condition on G of Eq. (A5) requires—even in the limit of a boundary at infinity—that the phase of the sine function have a definite value. This consideration leads directly to the expression for the density of normal modes given by Eq. (9), and also to the conclusion that the eigenvalue spectrum of the normal modes of a neutral Thomas-Fermi atom is continuous.

The constant k which appears in the biorthogonality relation between normal modes of velocity potential and normal modes of number density, Eq. (12), is also evaluated by use of the normalized asymptotic functions. Here one needs to calculate the normalization integral in the denominator of Eq. (13), the definition of the constant k . We imagine that the volume integration is done out to some large but finite radius x_0 which is in the asymptotic region. The remainder of the integration, out to the boundary, can be carried out using the asymptotic normalized functions G_N and H_N . In terms of the parameter x the integral becomes

$$\int N_{10}(\omega, \mathbf{r}) U_{10}(\omega, \mathbf{r}) d\mathbf{r} = \text{finite part} + A \int_{x_0}^{x_{\text{bound}}} \left[\frac{G^2}{x\varphi} + \frac{GH}{x^{7/4}\varphi^{1/4}} \right] x^2 dx,$$

where A is a collection of numerical constants. The second term in the integrand decreases rapidly enough so that its integral will be finite in the limit as the boundary goes to infinity. We simply add this contribution to the finite part already present. Substitution of the asymptotic function G_N in the remaining first term of the integrand gives an integrand of the form $\sin^2(\Phi + az) dz$, where $z = x^3/3$. We include the contribution from the lower limit with the “finite part,” take the average value of the square of the sine as $\frac{1}{2}$, and obtain

$$\int N_{10}(\omega, \mathbf{r}) U_{10}(\omega, \mathbf{r}) d\mathbf{r} = \text{finite part} + A' x_{\text{bound}}^3, \quad (\text{A8})$$

where A' is another, slightly different, collection of constants. This expression, inserted into Eq. (13), gives

$$k^{-1} = \lim_{x_{\text{bound}} \rightarrow \infty} \frac{(\hbar^3/m e^4 Z) (x_{\text{bound}}^3/2^6 \sqrt{3})}{\text{finite part} + A' x_{\text{bound}}^3}.$$

In the limit as the boundary goes to infinity the “finite part” of the denominator can be neglected and we obtain a finite ratio for k^{-1} . Its value after the numerical constants are reduced is

$$k^{-1} = [(2l+1)/4\pi] (m/\hbar Z^{2/3}) (3^4 \pi^4/2^5)^{1/3}, \quad (\text{A9})$$

a result which is independent of Ω . The dependence upon l is a consequence of our use of unnormalized Legendre functions. This feature imposes no difficulty

in our problem since we deal only with modes having dipole symmetry. If the angular dependence of the normal mode functions were expressed in terms of normalized spherical harmonics the constant k would be the same for all modes.

JWKB Solutions at Intermediate Distances

The asymptotic functions for G and H at large distances consist of the sum of a slowly varying function and a rapidly oscillating function. Eventually we shall integrate numerically the coupled second-order equations for G and H , starting at the origin and proceeding outward. As the integration proceeds G oscillates more and more rapidly. This behavior occurs well before the asymptotic region is reached. These rapid oscillations of G suggest that a good approximation to the solutions at intermediate distances can be obtained by using the JWKB method. The functions G and H are represented by a slowly varying amplitude function multiplied by a sine or cosine whose argument is given by an integral. In this type of solution G dominates. We assume for G the form,

$$G_{12} = \lambda^{-1/2} \left(\frac{\sin}{\cos} \right) \int^x \lambda(x) dx. \quad (\text{A10})$$

With this type of solution the amplitude is slowly varying so that to a good approximation we may write

$$G_{12}'' = -\lambda^2 G_{12}; \quad H_{12}'' = -\lambda^2 H_{12}.$$

Inserting these relations for the second derivatives into the set of coupled equations for G and H , Eq. (A3), we obtain

$$\begin{aligned} [\lambda(x)]^2 &= -\frac{1}{2}(GG) - \frac{1}{2}(HH) \\ &+ \frac{1}{2}\{[(GG) - (HH)]^2 + 4(GH)(HG)\}^{1/2} \\ &\approx -(GG) + \{(GH)(HG)/[(HH) - (GG)]\}. \end{aligned} \quad (\text{A11})$$

To find the corresponding solutions H_{12} we solve the equation of forced vibration,

$$H_{12}'' - (HH)H_{12} = (HG)G_{12}, \quad (\text{A12})$$

and obtain a first approximation of H_{12} ,

$$H_{12} = -[(HG/\lambda^2 + (HH)]G_{12}.$$

The coefficients of Eq. (A12) depend upon position so we must add to the first approximation a correction term which will be out of phase with G . We assume a better approximation for H ;

$$H_{12} = \{-(HG)/[\lambda^2 + (HH)]\}G_{12} + (\text{correction}),$$

insert it into Eq. (A12), and take the second derivative explicitly. Only terms containing the first derivative of the amplitude are retained, which gives an equation

for the correction term,

$$\begin{aligned} & (d^2/dx^2) (\text{corr.}) - (HH) (\text{corr.}) \\ & = 2G_{12}' (d/dx) [(HG)/\lambda^2 + (HH)]. \quad (\text{A13}) \end{aligned}$$

The derivatives of the oscillating functions are considered, in the spirit of the JWKB method, to be expressible in terms of the oscillating function itself, multiplied by a power of λ . Thus the corrected H is given by

$$\begin{aligned} H_{12} = & \frac{-(HG)\lambda^{-1/2}}{\lambda^2 + (HH)} \left(\frac{\sin}{\cos} \right) \int^x \lambda(x) dx \\ & - \frac{2\lambda^{1/2}}{\lambda^2 + (HH)} \frac{d}{dx} \left[\frac{(HG)}{\lambda^2 + (HH)} \right] \left(\frac{\cos}{\sin} \right) \int^x \lambda(x) dx. \quad (\text{A14}) \end{aligned}$$

So far we have obtained only two independent solutions in the intermediate region, those for which G is dominant and rapidly oscillating. The other two solutions are those for which H is dominant and has an exponential character. We again employ the JWKB method, only now using solutions of exponential type for H . We assume that H may be expressed in the form

$$H_{34} = k^{-1/2} \exp[\pm \int^x h(x) dx], \quad (\text{A15})$$

where again the second derivatives of G and H may be approximated as

$$H_{34}'' = h^2 H_{34}; \quad G_{34}'' = h^2 G_{34}.$$

These solutions are substituted into the coupled equations (A3) to give

$$\begin{aligned} h^2 = & (4x^2)^{-1} + \frac{1}{2}(GG) + \frac{1}{2}(HH) \\ & + \frac{1}{2}\{[(GG) - (HH)]^2 + 4(GH)(HG)\}^{1/2} \\ \approx & (4x^2)^{-1} + (HH) + \{(GH)(HG)/[(HH) - (GG)]\}, \end{aligned}$$

where we have added a term $1/4x^2$. This term is suggested by experience with JWKB solutions of the exponential type. For example, the JWKB approximation to the exact solution of the second-order equation,

$$x^2 y'' - l(l+1)y = 0,$$

is much improved if $l(l+1)$ is replaced by $(l + \frac{1}{2})^2$.

For the H dominant type of solution G is small and varies only slowly. We can therefore neglect the second derivative of G and obtain for the solutions G_{34} corresponding to H_{34} ,

$$G_{34} = [- (GH)/(GG)] k^{-1/2} \exp(\pm \int^x h(x) dx). \quad (\text{A16})$$

This set of four independent JWKB solutions, Eqs. (A10), (A14), (A15), (A16) provides a way calculating G and H in the region of intermediate and large distances where the rapid oscillations of the functions make accurate numerical integration difficult. We use

for G and H at intermediate distances a linear combination of these four solutions which (1) fits smoothly onto H and G as integrated outward from the origin, and (2) reduces at large distances to the normalized asymptotic forms of G_N and H_N .

Numerical Integration of H and G Outward from the Origin

Near the origin there is no convenient analytic expression for the Thomas-Fermi function. The coefficient (GG) changes sign, producing a turning point, so that the JWKB procedure is awkward. There is no alternative but numerical integration, at least for intermediate values of the frequency parameter Ω . Of the four boundary conditions needed to specify a unique solution, two boundary conditions have already been used to fix the behavior of H and G at large distances. The other two boundary conditions must be applied at the origin and must be chosen to give physically reasonable behavior there. We therefore consider the behavior of H and G at very small distance where the set of coupled equations, Eqs. (A3), becomes

$$\begin{aligned} G'' = & \{ [l(l+1)/x^2] - (3/16x^2) \} G - (27\pi^2 \Omega^2 x^{1/4}/256) H, \\ H'' = & \frac{3}{2} x^{1/4} G + \{ [l(l+1)/x^2] + (3/2x^{1/2}) \} H. \quad (\text{A17}) \end{aligned}$$

Here we have used the limiting value $\varphi(0) = 1$ for the Thomas-Fermi function at the origin. To find the leading term of a power series expansion about the origin we take $G \propto x^a$ and $H \propto x^b$. First assume that G is dominant— G drives H but H does not drive G . In this case the second of Eqs. (A17) requires that $b = a + 9/4$, and the first of Eqs. (A17) determines a and b ,

$$\begin{aligned} a = & \frac{1}{2} \pm \left[\frac{1}{16} + l(l+1) \right]^{1/2} \\ b = & \frac{1}{4} \pm \left[\frac{1}{16} + l(l+1) \right]^{1/2}. \end{aligned}$$

The opposite assumption that H is dominant requires that $a = b + 9/4$ and that

$$\begin{aligned} a = & \frac{9}{4} - l, \quad \frac{9}{4} + (l+1) \\ b = & -l, \quad l+1. \end{aligned}$$

The general solution near the origin can thus be written as a linear combination of four solutions,

$$\begin{aligned} G = & e_1 x^{1.936} + e_2 x^{-0.936} - e_3 3.33/\Omega^2 x^{1.25} - e_4 0.07536 \Omega^2 x^{4.25} \\ H = & e_1 0.1125 x^{4.186} + e_2 3.6355 x^{1.314} + e_3 x^{-1} + e_4 x^2. \end{aligned}$$

Here we have explicitly used the value $l=1$. For each of the four independent solutions the driving equation determines a definite ratio of the constants of proportionality in the power law approximation of G and H . These ratios appear above as numerical coefficients of the subdominant functions.

In order clearly to see which of the linearly independent solutions represent physically acceptable behavior near the origin we examine what each implies for the physical normal mode functions n_1 , U_1 , and V_1 .

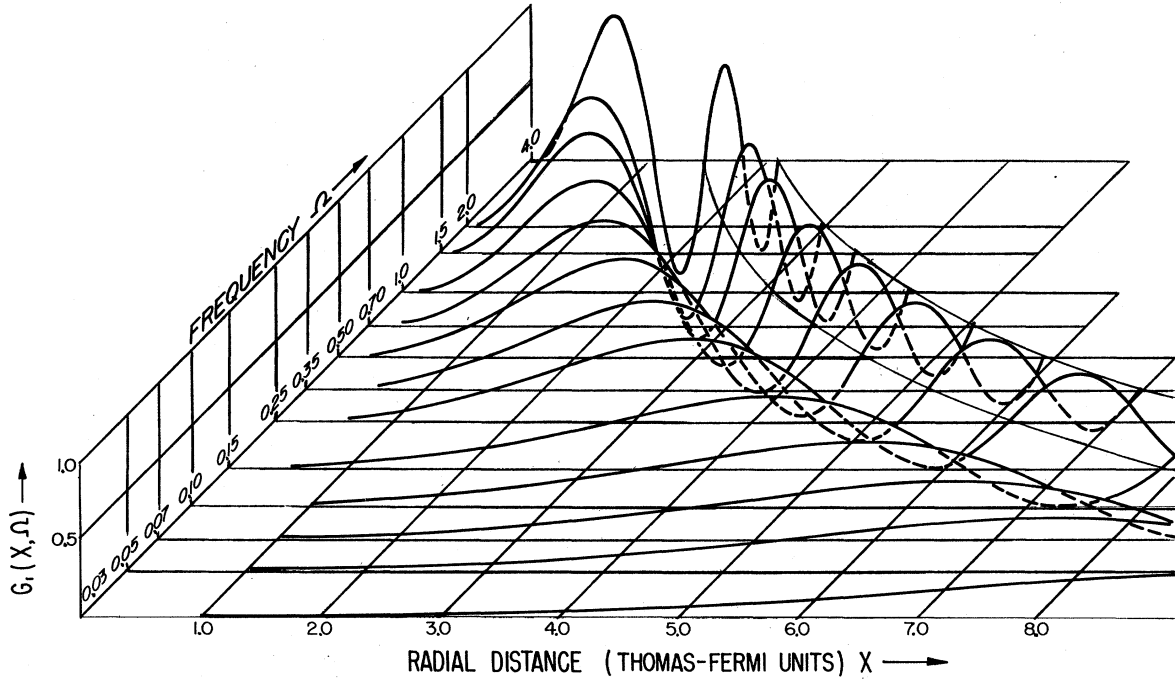


FIG. 3. A plot of the normalized velocity potential function, $G_1(x, \Omega)$, for the dipole mode ($l=1$) of oscillation of the Thomas-Fermi atom. Here and in Fig. 4 each function is represented by a series of vertical cross sections through a two-dimensional surface whose height is a continuous function of x and Ω . The radial distance x is in Thomas-Fermi units where $x = (m\epsilon^2/\hbar^2)(128Z/9\pi^2)r$. The frequency $\Omega = (\hbar\omega \text{ eV})/(27.2Z \text{ eV})$. The frequency is plotted on a logarithmic scale in the oblique direction. Each curve is a numerically calculated function at a given frequency, plotted without distortion.

Table II summarizes the situation for the mode of dipole symmetry $l=1$ in which we are interested. The solution G_2, H_2 must be discarded because it leads to a number density of electrons near the origin which diverges more strongly than the equilibrium number den-

TABLE II. Behavior at small radial distance of the four independent solutions of the coupled equations which determine the dipole modes of oscillation; cf. Appendix A, Eq. (A17) ff. Radial distance is proportional to x .

	Behavior of G and H	Behavior of physical normal mode functions
G Dominant	$G_1 \propto x^{1.93614}$	$n_1 \propto x^{1.18614} + x^{2.68614}$
	$H_1 \propto x^{4.18614}$	$U_1 \propto x^{1.68614}$
	$G_2 \propto x^{-0.93614}$	$V_1 \propto x^{3.18614}$
	$H_2 \propto x^{1.31386}$	$n_1 \propto x^{-1.68614} + x^{-0.18614}$
		$U_1 \propto x^{-1.18614}$
		$V_1 \propto x^{0.31386}$
H Dominant	$G_3 \propto x^{5/4}$	$n_1 \propto x^{1/2} + x^{-5/2}$
	$H_3 \propto x^{-1}$	$U_1 \propto x$
		$V_1 \propto x^{-2}$
	$G_4 \propto x^{27/4}$	$n_1 \propto x^{7/2} + x^{1/2}$
	$H_4 \propto x^2$	$U_1 \propto x^4$
		$V_1 \propto x$

For the equilibrium Thomas-Fermi atom: $n_0 \propto x^{-3/2}, V_0 \propto x^{-1}, U_0 = 0$.

sity n_0 . The assumption that the normal mode is a small fluctuation breaks down near the origin for this type of solution. We must also discard the solution G_3, H_3 since it leads to a potential energy per electron near the origin which behaves as x^{-2} , a more rapid divergence than the coulomb potential. We exploit the fact that one of the two acceptable solutions is a G dominant type while the other acceptable solution is an H dominant type. Explicitly, we have

$$G = e_1 x^{1.936} - e_4 0.07536 \Omega^2 x^{4.25}$$

$$H = e_1 0.1125 x^{4.186} + e_4 x^2.$$

At small distances the terms with numerical coefficients fall off so much faster than the terms without numerical coefficients that one can neglect them and write

$$G \simeq e_1 x^{1.936}, \quad H \simeq e_4 x^2.$$

For our purposes it proves more convenient to take as two basic solutions in the small- x regime, not the solutions given by $(e_1=1, e_4=0)$ and $(e_1=0, e_4=1)$, but the following linear combinations thereof,

$$\begin{aligned} G_+ &= x^{1.93614} & H_+ &= x^2 \\ G_- &= x^{1.93614} & H_- &= -x^2. \end{aligned} \quad (\text{A18})$$

The final normalized solutions for H_N and G_N will be some linear combination of $+$ and $-$ solutions which

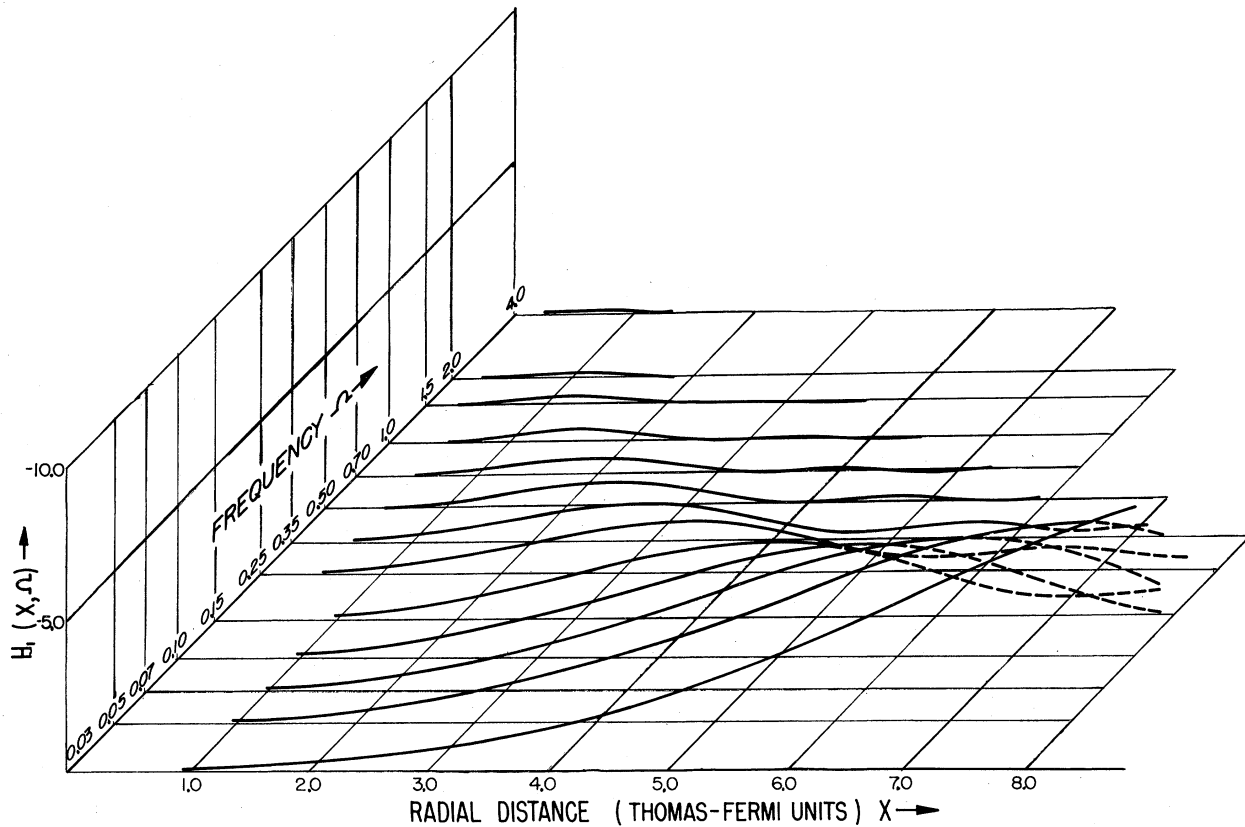


FIG. 4. A plot of the normalized potential energy function, $H_1(x, \Omega)$, for the dipole mode ($l=1$) of oscillation of the Thomas-Fermi atom. The plot follows the plan of Fig. 3.

start near the origin with these power laws

$$\begin{aligned} G_N &= k_+ G_+ + k_- G_- \\ H_N &= k_+ H_+ + k_- H_- \end{aligned} \quad (\text{A19})$$

The constants, as yet undetermined, must be chosen so that the solutions integrated outward from the origin satisfy the boundary condition at infinity.

Fitting the Solutions

We have discussed the behavior of the functions H and G in three regions: (1) near the origin, (2) at intermediate distances, and (3) in the asymptotic region. It remains to describe the procedure for fitting together the solutions from the various regions into the final normalized solutions G_N and H_N .

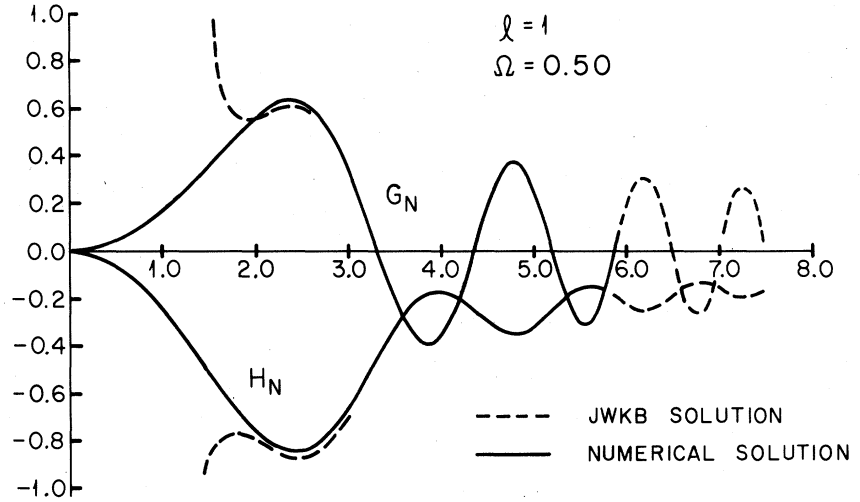
For a given value of Ω the coupled second-order Eqs. (A3) are integrated numerically out to a value of x which is well within the region where the JWKB type of solution is good. This is done for both the $+$ solution and the $-$ solution, using the power laws, Eqs. (A18), to establish the starting values. The rapidity of the oscillations which develop is a strong function of frequency Ω so we use a finer numerical grid for higher

values of Ω . The procedure of numerical integration is that described by Fox and Goodwin (1949), modified for the case of two coupled equations. This integration procedure takes into account central differences of the fourth order initially and includes a method of correcting the functions obtained to include the effects of higher-order differences. In our calculation the numerical grid was fine enough so that central differences of the sixth order were random in sign. Sixth- and higher-order differences were consequently neglected since their inclusion would not improve the accuracy.

As a next step the eight JWKB solutions, four for each of the functions H and G , are evaluated in a region which overlaps the numerically computed solutions and which extends out to radial distances at which the functions oscillate very rapidly. The arbitrary lower limit of the phase integrals is chosen for convenience at the beginning of the region in which the JWKB solutions are calculated.

Two points x_1 and x_2 with an approximate separation of $3\pi/2$ in the phase of the JWKB solution are chosen in the region of overlap. The requirement that the numerically integrated solution match the JWKB solution at these two fitting points determines a unique

FIG. 5. A typical example of the fitting between numerical solutions and JWKB solutions, illustrated for the case of the dipole mode ($l=1$) of frequency $\Omega=0.5$. The abscissa is radial distance x in Thomas-Fermi units.



linear combination of JWKB solutions which continues the numerical solution. For example, to continue the + solution we solve the set of equations,

$$G_+(x_1) = \sum_i c_i^+ G_i(x_1),$$

$$G_+(x_2) = \sum_i c_i^+ G_i(x_2),$$

$$H_+(x_1) = \sum_i c_i^+ H_i(x_1),$$

$$H_+(x_2) = \sum_i c_i^+ H_i(x_2),$$

for the four unknown coefficients c_i^+ , where $i=1, 2, 3, 4$. An analogous set of equations is solved for the four unknown coefficients c_i^- which determines the linear combination of JWKB solutions that continues the - type of numerical solution into the JWKB region. In the JWKB region the normalized solution will thus be the linear combination,

$$G_N = \sum_i (k_+ c_i^+ + k_- c_i^-) G_i$$

$$H_N = \sum_i (k_+ c_i^+ + k_- c_i^-) H_i,$$

where the constants k_+ and k_- have yet to be determined.

One of the JWKB solutions H_3, G_3 is an unstable one, exponentially increasing with distance, which can never satisfy the boundary condition at infinity. Furthermore this solution continues in the JWKB region the unstable part of the numerically integrated functions, a part which unavoidably appears because of small errors in the step-by-step numerical integration. We satisfy the boundary condition at infinity and simultaneously eliminate the unstable part of the numerical solution by setting the coefficient of H_3 and G_3 equal to zero; i.e.,

$$k_+ c_3^+ + k_- c_3^- = 0. \quad (\text{A20})$$

A final condition on the k 's is the requirement that the oscillating part of the JWKB solution have the same amplitude at very large distances as the asymptotic form of Eq. (A7). This condition, which fixes the normalization, is

$$\begin{aligned} & [(k_+ c_1^+ + k_- c_1^-)^2 + (k_+ c_2^+ + k_- c_2^-)^2]^{1/2} \\ &= [\lambda(x)]^{1/2} 2^2 / 3^{1/4} \pi^2 x = \Omega^{1/2}. \quad (\text{A21}) \\ & \lim_{x \rightarrow \infty} \end{aligned}$$

Equations (A20) and (A21) suffice to determine the k 's and thus to determine the normalized functions G_N and H_N both near the origin and at large distances. The normalized functions G_N and H_N for the dipole mode of oscillation are plotted in Figs. 3 and 4, which show their behavior for several values of the frequency parameter in the range $0.03 < \Omega < 4.0$. For clarity only the first few oscillations of the functions are plotted.

The JWKB approximation gives a very accurate extension of the numerically computed functions. In the region of overlap the JWKB solutions coincide very well with the numerically integrated functions, only departing significantly near the first maximum of G and H . This behavior is illustrated for a typical set of coupled functions in Fig. 5. Throughout our analysis we have systematically separated the solutions into a G dominant and an H dominant part. The behavior of the coefficients of the coupled equations permits this and thus enables the JWKB procedure—normally applicable only to a single second-order differential equation—to be applied to the system of two coupled second-order equations. In turn the existence of the JWKB solutions permits the solutions near the origin to be connected to the asymptotic solutions. Only in this manner can we determine a unique solution which satisfies the boundary conditions both at the origin and at infinity.

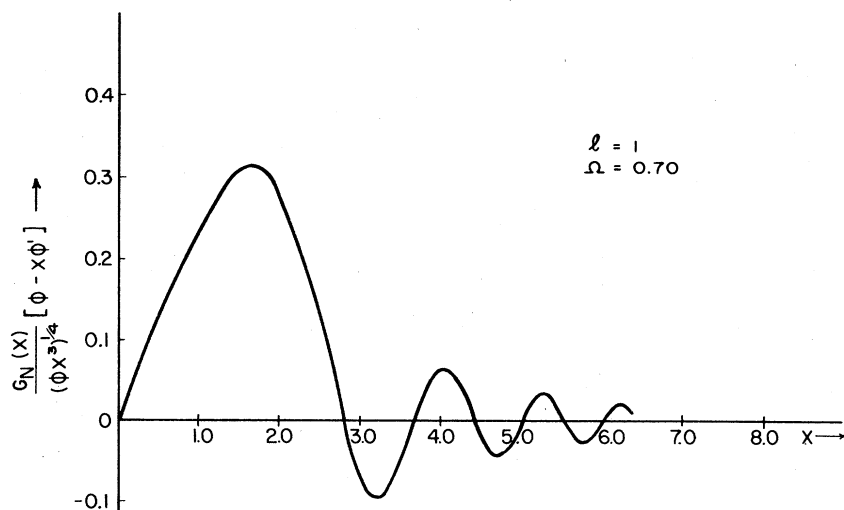


FIG. 6. Illustrating the rapid convergence of the dipole integral, Eq. (B2).

$$D(\Omega) = \int_0^\infty G_N(x) (\Phi x^3)^{-1/4} (\Phi - x\Phi') dx.$$

The integrand is plotted as a function of x in Thomas-Fermi units. The amplitude of the oscillating integrand decreases rapidly. The principal contribution to the dipole integral comes from the vicinity of the first maximum of G_N .

APPENDIX B: EVALUATION OF THE DIPOLE INTEGRAL

Intermediate Frequencies

Once the normalized functions H_N and G_N are obtained, they are used to evaluate the dipole integral which determines the photoabsorption cross section. The dipole integral over the fluctuation in number density of electrons is more easily evaluated when it is written in terms of the fluctuation of the velocity potential. The normal mode of the velocity potential is given by the dimensionless velocity potential factor G_N . Thus, by Eqs. (22) and (A2), we have

$$\int z N_{10}(\omega, \mathbf{r}) d\tau = \Omega^{-2} (\hbar^3 / m e^4) (\hbar^2 / m e^2) (4 / 3\pi Z)^{2/3} \times \int_0^\infty (\varphi x^3)^{-1/4} G_N(x) (\varphi - x\varphi') dx. \quad (B1)$$

The integrand in the above expression oscillates with rapidly decreasing amplitude. Its behavior for a typical frequency is shown in Fig. 6. The value of the dimensionless integral in Eq. (B1) above is calculated by the following procedure. The integral is done numerically out to some node of the integrand. The succeeding positive and negative loops of the integrand are then integrated separately. In this manner we can write the dimensionless integral, which we denote by $D(\Omega)$, as

$$D(\Omega) = \int_0^{x_{\text{node}}} (\varphi x^3)^{-1/4} G_N(x) (\varphi - x\varphi') dx + i_1 - i_2 + i_3 - \dots, \quad (B2)$$

where the i 's represent the contribution of each successive loop to the total integral. The Euler sum procedure is then used to sum the convergent alternating series of the i 's. Only the first several i 's are needed to obtain an accurate sum of the series.

The dimensionless integrals $D(\Omega)$, together with the value of the normalization constant k computed in Appendix A are substituted into Eq. (21) to obtain our final formula for the photoabsorption cross section,

$$\sigma(\Omega) = (3\pi\alpha a_0^2 / \Omega^2) [D(\Omega)]^2, \quad (B3)$$

where α is the fine structure constant and a_0 is the Bohr radius.

In this way we have calculated the universal photoabsorption cross section of Fig. 1. The solid dots indicate the points which were computed numerically. The values of the cross sections are also listed in Table I.

In order to estimate the accuracy of the computed cross sections it is necessary to examine the integration procedure which was used. The single most important factor is the length of the interval of radial distance, Δx , which was used both for the numerical integration of the differential equations and for the evaluation of the integrals of the functions. In order to determine the effect of different intervals Δx at different frequency ranges, we calculated the dipole integral $D(\Omega)$ at pairs of values of Ω which were close together but between which the computer program in use changes the integration interval by a factor of at least two in all cases. The situation is summarized by the following table:

Ω	$D(\Omega)$	% Difference of $D(\Omega)$
0.07	0.1554	2.2
0.0701	0.1520	
1.50	0.591	2.4
1.501	0.577	
4.00	0.688	16.0
4.01	0.798	

We conclude that within the range $0.03 < \Omega < 4.0$ the dipole integral is affected no more than 2.5% by a change in the interval of integration. Therefore the computational error of the photoabsorption cross sec-

tion in this range is estimated not to exceed about 4%. At higher frequencies the calculated cross section is much less accurate. At these frequencies, $4.0 < \Omega < 12.0$, the functions oscillate rapidly and rise steeply from the origin. The irregularity of the cross sections may be due either to the use of too large an interval of integration or to the inadequacy of using only a single term in the power series to obtain starting values of the functions near the origin. Consequently we conclude that the values of the cross section listed in Table I for the frequencies $4.0 < \Omega < 12.0$ may contain a computational error of about 15%.

A final check on the accuracy of the photoabsorption cross section is provided by the dipole sum rule which should be exactly satisfied for our model. Here we find that the integrated cross section checks the theoretical sum rule value to within 2%.

Limiting Forms of the Cross Section at Extremes of Frequency

When we pass from medium values of the frequency parameter Ω to very high and very low frequencies we find the desired hydrodynamic solutions more readily by analytic means than by numerical calculation. We are interested not so much in the solutions themselves as in what they predict for the photoabsorption cross section. The dipole integral for photoabsorption Eq. (B2) will be dominated by the contribution from values of x which lie near the first maximum of G . Consequently we have to determine correctly the course of the solution, not everywhere, but only near the first maximum. This maximum lies in the region of the atom where the Thomas-Fermi function φ is known only numerically so long as Ω is in the realm of intermediate frequencies. But at very high frequencies the maximum moves in close to the origin, where $\varphi \approx 1$; and at very low frequencies the principal maximum lies exceedingly far out, where $\varphi \approx 144/x^3$. Both expressions for φ permit us to obtain G in closed analytic form.

Near the origin at high frequencies, the coupled equations for G and H of index $l=1$ may be written

$$G'' = \left(\frac{29}{16x^2} - \frac{27\pi^2\Omega^2x}{256} \right) G - \frac{27\pi^2\Omega^2x^{1/4}}{256} H,$$

$$H'' = \frac{3}{2}x^{1/4}G + (2/x^2)H.$$

The coefficient (GG) is dominant, so neglecting other terms, we can obtain an approximate equation for G alone

$$G'' + [(27\pi^2\Omega^2x/256) - (29/16x^2)]G = 0. \quad (B4)$$

Only the function G is required in order to evaluate the absorption cross section. We introduce a new independent variable,

$$y = (3^{1/2}\pi\Omega x^{3/2})/2^3,$$

which reduces Eq. (B4) to a Bessel equation which

has the solution

$$G(y) = y^{1/3}J_g(y), \quad (B5)$$

where $g = (33)^{1/2}/6$. This Bessel function is regular at the origin and thus satisfies the boundary conditions there. In order to normalize this solution we compare it with the normalized asymptotic solution G_N . At intermediate distances and at high frequencies a JWKB solution for G which reduces to the canonically normalized G_N at large distance is

$$G_N = [4/(3^{3/4}\pi^{1/2})](\phi^{1/4}x) \times \sin [\text{const} + \int^x (3^{1/2}\pi\Omega/2^4)(x/\phi^{1/2}) dx].$$

Very near the origin this transitional solution becomes

$$G_N = [4/(3^{3/4}\pi^{1/2}x^{1/2})] \sin [\text{const} + (3^{1/2}\pi\Omega x^{3/2}/2^8)]. \quad (B6)$$

Comparison of Eq. (B6) with the asymptotic form of the Bessel function solution Eq. (B5) furnishes the proper normalization. For the normalized G at high frequencies we obtain

$$G_N(x) = (2\pi^{1/6}\Omega^{1/6}/3^{2/3})y^{1/3}J_g(y). \quad (B7)$$

This solution peaks at $y \approx 1$ and for large y oscillates with ever decreasing amplitude. Thus the contribution to the absorption comes only from y values approximately equal to 1, or only from x values of about $x \approx \Omega^{-2/3}$. Thus for high frequencies one can replace $(\varphi x^3)^{-1/4}(\varphi - x\varphi')$ in the interaction integral Eq. (B2) by $x^{-3/4}$ and have the integral reduce to the limiting form

$$D(\Omega) = \int_0^\infty [G_N(x)/x^{3/4}] dx$$

$$= (2^{5/2}/3^{7/4}) \int_0^\infty y^{-1/2}J_g(y) dy = 0.805.$$

We substitute this result into Eq. (B3) and obtain the limiting form of the cross section at high frequencies

$$\sigma(\Omega) = [1.242(10)^{-18}/\Omega^2] \text{ cm}^2. \quad (B8)$$

In the opposite case of extremely low frequencies the first maximum lies at extremely large x , where $\varphi = 144/x^3$. The differential equations for H and G take the limiting form

$$G'' = [(8/x^2) - (3\pi^2\Omega^2x^4/2^{12})]G - (3^{5/2}\pi^2\Omega^2x/2^9)H,$$

$$H'' = (3^{1/2}x/4)G + (20/x^2)H.$$

Again the coefficient of G in the first equation dominates and G drives itself and is influenced very little by H . We neglect this small coupling and consider only the equation for G ,

$$G'' + [(3\pi^2\Omega^2x^4/2^{12}) - (8/x^2)]G = 0. \quad (B9)$$

The JWKB solution for G_N in the asymptotic region

suggests the change of variable,

$$y = (\pi\Omega x^3)/(3^{1/2}2^6),$$

which reduces Eq. (B9) to a Bessel equation with the acceptable solution,

$$G(x) = y^{1/6} J_0(y).$$

Again we have $g = (33)^{1/2}/6$. We compare the asymptotic form of this Bessel function with the normalized solution G_N . This procedure furnishes the normalized solution at low frequencies

$$G_N(x) = (\pi\Omega x/6)^{1/2} J_0[(\pi\Omega x^3)/(3^{1/2}2^6)]. \quad (\text{B10})$$

Inserting this solution into Eq. (B2), and using the asymptotic form of φ , we obtain

$$D(\Omega) = (\pi\Omega^{3/2}/3^{1/4}) \int_0^\infty y^{-3/2} J_0(y) dy = (\pi\Omega/3^{1/4}) (4.36).$$

*Research supported by the U.S. Atomic Energy Commission under Contract No. AT(30-1)-937 and by the Higgins Scientific Trust Fund and in part by N.S.F. Grant GP-30799X to Princeton University.

†This work is included in: J.A. Ball, Ph.D. thesis, Princeton 1963 (unpublished).

‡Present address: Mission Research Corporation, Santa Barbara, Calif.

§Present address: Smithsonian Inst., 60 Garden St., Cambridge, Mass.

Afrosimov, V. V., Y. S. Gordeev, M. N. Panov, and N. V. Fedorenko, 1964, *Zh. Tekh. Fiz.* **34**, 1624.

Bethe, H. A., 1930, *Ann. Phys. (Leipzig)* **5**, 325.

Bethe, H. A., 1933, *Handb. Phys.* **24**, 523.

Bloch, F., 1933, *Z. Phys.* **81**, 363.

Bohr, A., 1948, *K. Dan. Vidensk. Selsk. Mat.-Fys. Medd.* **24** (19).

Bohr, N., 1948, *K. Dan. Vidensk. Selsk. Mat.-Fys. Medd.* **18** (8).

Brandt, W., and S. Lundqvist, 1965, *Phys. Rev.* **139**, A612.

Brandt, W., and S. Lundqvist, 1965a, *Ark. Fys.* **28**, 399.

Breit, G., and S. Korff, 1932, *Rev. Mod. Phys.* **4**, 471.

Fano, U., 1963, *Annu. Rev. Nucl. Sci.* **13**, 1.

Fano, U., and J. W. Cooper, 1968, *Rev. Mod. Phys.* **40**, 441.

This value of the dipole integral yields the cross section,

$$\sigma(\Omega) = 207.5(10)^{-18} \text{ cm}^2, \quad (\text{B11})$$

a result which is independent of frequency. Of course this result is a limiting value as Ω approaches zero. To determine how far Ω may depart from zero before $\sigma(\Omega)$ becomes significantly different from this constant value, we must examine the conditions for which the above calculation is applicable. A condition for Eq. (B11) to be valid is that the turning point in Eq. (B9) be in the asymptotic region. This condition may be met by requiring the turning point to be at a distance $x=100$, which results in a frequency $\Omega=3(10)^{-5}$. Therefore this value of frequency can be taken as the rough upper limit for which Eq. (B11) is applicable.

Both limiting results, at very high frequencies and at very low frequencies, cannot be expected to be realistic physically. The hydrodynamic model itself is not valid at these extremes of frequency.

Fermi, E., 1928, *Z. Phys.* **48**, 73.

Fox, L., and E. T. Goodwin, 1949, *Proc. Camb. Philos. Soc.* **45**, 373.

Goldstone, J., and K. Gottfried, 1959, *Nuovo Cimento* **13**, 849.

Gombas, P., 1956, *Handb. Phys.* **36**, 109.

Inokuti, M., 1971, *Rev. Mod. Phys.* **43**, 297.

Kirzhnits, D. A., and Yu. E. Lozovik, 1966, *Usp. Fiz. Nauk* **89**, 39.

Lindhard, J., 1954, *K. Dan. Vidensk. Selsk. Mat.-Fys. Medd.* **28** (8).

Lindhard, J., and M. Scharff, 1953, *K. Dan. Vidensk. Selsk. Mat.-Fys. Medd.* **27** (15).

March, N. H., 1951, *Adv. Phys.* **6**, 1.

Nozieres, P., and D. Pines, 1958, *Nuovo Cimento* **9**, 470.

Samson, J. A. R., 1966, *Adv. At. Mol. Phys.* **2**, 177.

Sen, A., and E. G. Harris, 1971, *Phys. Rev. A* **3**, 1815.

Sziklas, E. A., 1965, *Phys. Rev.* **138**, A1070.

Thomas, L. H., 1926, *Proc. Camb. Philos. Soc.* **23**, 524.

Weidner, S., and S. Borowitz, 1966, *Phys. Rev. Lett.* **16**, 722.

Wheeler, J. A., and R. Landenburg, 1941, *Phys. Rev.* **60**, 761.

Wheeler, J. A., and E. L. Fireman, 1957, "A Universal Photo-Absorption Curve," Aeronutronic Systems, Inc., ASI Publication No. U-099, December 17, 1957.